HHS Public Access

Author manuscript

Cancer Lett. Author manuscript; available in PMC 2023 September 01.

Published in final edited form as:

Cancer Lett. 2022 September 01; 543: 215779. doi:10.1016/j.canlet.2022.215779.

Versican secreted by the ovary links ovulation and migration in fallopian tube derived serous cancer.

Angela Russo[1], **Yang Zizhao**[1], **Georgette Moyle Heyrman**[2], **Brian P. Cain**[3], **Alfredo Lopez Carrero**[1], **Brett C. Isenberg**[3], **Matthew J. Dean**[4], **Jonathan Coppeta**[3], **Joanna E. Burdette**[1,*]

[1]Department of Pharmaceutical Sciences, University of Illinois at Chicago, Chicago, IL, 60607

[2]Department of Chemistry, University of Wisconsin, Green Bay, WI, 54311

[3]Charles Stark Draper Laboratory, Cambridge, MA, 02139

[4]Department of Animal Sciences, University of Illinois Urbana-Champaign, Urbana, IL, 61801

Abstract

High grade serous ovarian cancers (HGSOC) predominantly arise in the fallopian tube epithelium (FTE) and colonize the ovary first before further metastasis to the peritoneum. Ovarian cancer risk is directly related to the number of ovulations, suggesting that the ovary may secrete specific factors that act as chemoattractants for fallopian tube derived tumor cells during ovulation. We found that 3D ovarian organ culture produced a secreted factor that enhanced the migration of FTE non-tumorigenic cells as well as cells harboring specific pathway modifications commonly found in high grade serous cancers. Through size fractionation and a small molecule inhibitors screen, the secreted protein was determined to be 50–100kDa in size and acted through the Epidermal Growth Factor Receptor (EGFR). To correlate the candidates with ovulation, the PREDICT organ-on-chip system was optimized to support ovulation in a perfused microfluidic platform. Versican was found in the correct molecular weight range, contained EGF-like domains, and was found to correlate with ovulation in the PREDICT system. Exogenous versican increased migration, invasion, and enhanced adhesion of both murine and human FTE cells to the ovary in an EGFR-dependent manner. The identification of a protein secreted during ovulation that impacts the ability of FTE cells to colonize the ovary provides new insights into the development of strategies for limiting primary ovarian metastasis.

Keywords

Versican; migration; fallopian tube; ovulation; EGFR

*To whom correspondence should be addressed.

Author contributions

AR, YZ, AL, MD, GH and BC contribute with data and/or figures. AR wrote the paper and prepared the figures. JC, BI and JB supervised the project.

Conflict of interests

The authors declare they have no conflicts of interests.

Introduction

High grade serous ovarian cancer (HGSOC) is the most common and deadly histologic subtype of ovarian cancer (2) and contributes to approximately 14,000 deaths each year in the U.S. (3). Increasing evidence supports that HGSOC originates from malignant transformation of the FTE that generate precursors lesions called serous tubal intraepithelial carcinoma (STIC)(4, 5). Risk reducing salpingectomy protects against developing ovarian cancer (6) and high-risk patients often harbor p53 mutations and lesions in their fallopian tubes prior to developing HGSOC. Ovulation is a risk factor for developing ovarian cancer (7), and this suggests that the ovary may play an important role potentially in the transformation, metastasis, and proliferation of fallopian tube epithelial (FTE) derived cancers. Ovulation ends at the time of menopause, which is the period when most ovarian cancers are detected, primarily because there are no early detection strategies for ovarian cancer. Tumor initiation of high-grade serous cancer has been shown through evolutionary analyses to begin as a p53 signature, followed by a STIC lesions with an estimated window of 7–20 years before widespread metastases are detected (8). Exposure of the FTE to follicular fluid released at the time of ovulation increases DNA damage, recruits pro-inflammatory macrophages, and triggers p53 accumulation, a hallmark of precursor lesions (9, 10). In this study, we uncovered specific ovarian factors that are produced in response to ovulation using organ-on-a-chip technology and we characterized the ovarian factors as key mediators of fallopian tube cell migration, invasion, and adhesion to the ovary as part of primary metastasis.

High grade serous tumors that arise in the fallopian tube frequently spread to the ovary and proliferate into a large tumor mass (11, 12). A few ovarian proteins have been reported to impact the FTE by increasing tumorigenic properties and potentially enhancing metastasis of FTE cells to the ovary. For example, stromal cell-derived factor 1 (SDF-1), a component of follicular fluid, increased metastasis of stem-like ovarian cancer cells to the ovary and other peritoneal sites (13). Activin A, an ovarian peptide hormone, induced an epithelial-to-mesenchymal transition (EMT) and stimulated migration of murine oviductal cells (14). Norepinephrine production in the ovary is specifically enhanced when fallopian tube cells become tumorigenic and it stimulates colonization of the ovary (15, 16). Ovarian brain-derived neurotropic factor (BDNF) induced mutant p53 expressing fallopian tube cell migration (17, 18). Importantly, none of these have been profiled for their abundance and relationship to ovulation, which has been made possible through bioengineering strategies to mimic ovulation using microfluidic organ-on-a-chip technologies (19). Furthermore, the previous studies focus primarily on factors made by the ovarian follicle rather than using an organ-based approach.

Versican is a large proteoglycan involved in different aspects of ovarian cancer progression, such as migration, invasion, apoptosis, angiogenesis, and morphogenesis (20–23). Expression of versican in the stromal cells of the ovary is associated with invasive carcinoma (24). Versican accelerated ovarian cancer metastasis *in vivo* (25). Reduction of versican expression attenuated epithelial ovarian carcinoma spheroid formation, reduced cell adhesion to peritoneal mesothelial cell monolayers, and alleviated peritoneal tumor formation (13). Versican interacts with hyaluronan (HA) and binds to CD44 receptors

to impact extracellular matrix (ECM) integrity thereby driving cellular adhesion and the metastasis of cancer cells, including ovarian cancer (21, 22). Versican's G3-domain, which contain EGF-like motifs, mediates breast tumorigenesis, invasiveness, and metastasis (26).

In the present study, we demonstrated that an ovarian secreted factor increased FTE migration in an EGFR-dependent manner. We employed a state-of-the-art microfluidic device that allowed *ex vivo* ovulation of murine ovaries and showed increased versican secretion during a periovulatory phase. Versican enhanced MOE and FTE migration, invasion, and adhesion to the ovary, which was blocked by EGFR inhibitors. Together, these data suggest that versican is an ovarian signal regulated during ovulation that enhances fallopian tube cancer cell colonization of the ovary.

RESULTS

Ovarian conditioned media contains secreted proteins that increases fallopian tube cells migration.

The ovary is a primary site of metastasis for fallopian tube-derived high grade serous cancer. Studies have demonstrated that cancer cells injected intravenously in mice home to the ovary (27) and our previous work found that cells allografted inside the murine ovarian bursa, near the ovary, developed aggressive cancer that spreads to the peritoneal space, suggesting that the ovary exacerbated cancer progression (28). A 3D ovarian alginate culture was used to collect secreted ovarian factors in the conditioned medium (10). Ovarian conditioned media was added to murine oviductal epithelial cells (MOE, the mouse equivalent of human fallopian tube epithelium) and immortalized non-tumorigenic human fallopian tube epithelial cells (FT33-TAg). Ovarian conditioned medium generated a significant increase in the migration of MOE and FT33-Tag cells as measured using a wound healing assay (Fig. 1A, Supp. Fig1A and Supp. Fig. 2A). Conditioned media from the oviduct only increased migration in MOE but not in FT33-TAg (Supp. Fig. 2B, 2C). Conditioned media from the ovary and the oviduct also increased proliferation of MOE (Supp. Fig. 2D).
To further characterize the conditioned media components that were responsible for the increased migration, the conditioned medium was heated to denature proteins or treated with proteinase K to digest proteins. Both treatments reduced the pro-migratory action of the conditioned medium suggesting that the secreted factor was a protein (Fig. 1B, C and Supp. Fig 1B, C). Size fractionation further confirmed that the factor was a protein, and not a small molecule or hormone, since only the fraction with factors that were larger than 3kDa increased migration (Fig. 1D and Supp. Fig 1D). Additional size fractionation indicated that the protein that increased migration had a size range of 50–100kDa (Fig. 1E). We performed mass spectrometry-based proteomics on the conditioned media from the ovary and the fallopian tube and found that ovarian conditioned media contained about 600 proteins, while the fallopian tube only secreted only about 90 proteins, which is illustrated by the Venn diagram in Fig. 1F. In addition, we mined the data using software to predict secreted proteins and focused on proteins that are known to be secreted (Fig. 1G).

Ovarian conditioned media increased cell migration in oviductal models of early tumorigenesis.

We have developed stable cell lines from murine oviductal epithelium that model common pathways impacted in high grade serous cancer (29). In these models, loss of PTEN or mutation of TP53 in MOE cells increased migration (30, 31) as compared to wild-type cells. To address how secreted ovarian proteins impact fallopian tube models of disease, MOE cells expressing mutant $TP53^{R248W}$, $TP53^{R273H}$, $KRAS^{G12V}$, $PTEN^{shRNA}$, $PTEN^{shRNA}$+$TP53^{R273H}$, or $PTEN^{shRNA}$+$KRAS^{G12V}$ were exposed to ovarian conditioned medium. The MOE cells expressing the $TP53^{R248W}$ only (Fig. 2A) or mutation of $KRAS^{G12V}$ only (Fig. 2C) did not respond to conditioned media, whereas a significant increase in migration was found in oviductal cells expressing $TP53^{R273H}$ (Fig. 2B), $PTEN^{shRNA}$ (Fig. 2D), $PTEN^{shRNA}$+$TP53^{R273H}$ (Fig. 2E), or $PTEN^{shRNA}$+$KRAS^{G12V}$(Fig. 2F). These results suggest that specific pathway alterations that occur during tumorigenesis impact the response to ovarian secreted factors.

Ovarian conditioned media increased migration of murine and human fallopian tube epithelial cells in an EGFR-dependent manner.

To further define which proteins in the ovarian conditioned media were contributing to the increased migratory phenotype, we performed a DAVID analysis of protein domains, which revealed a high number of proteins with EGF-like domains in the conditioned medium (Fig. 3A). However, EGF itself was not found in the conditioned medium based on proteomics. MOE and FT33-Tag cells express the EGF receptor (EGFR) (Fig. 3B) and responded to recombinant EGF by significantly increasing migration (Fig. 3C and Supplemental Fig. 3A). Furthermore, MOE cells were treated with a small set of inhibitors involved in regulating pro-migratory pathways in including a CXCR4/SDF-1(CXCL12) inhibitor (AMD3100), a matrix metalloprotease inhibitor (GM6001), an autocrine motility factor (AMF) inhibitor (E4P), a TGF-β receptor inhibitor (SB431542), and an EGFR inhibitor (PD158780) (Supp. Fig. 4A–C and F). Only inhibition of CXCR4/SDF-1(CXCL12) and EGFR reduced the conditioned media pro-migratory effect (Supp. Fig. 4D-F). However, recombinant SDF-1 did not increase migration (Supp. Fig. 2E) suggesting that other factors in the conditioned media may be required for CXCR4 activation. In both FT33-TAg and in MOE cells the EGFR inhibitor at 1μM and 10μM blocked migration from ovarian conditioned medium (Fig. 3D–G and Supplemental Fig. 3B–C).

Proteomic analysis identified the proteoglycan versican as a potential candidate for the CM-induced effects

The 50–100kDa fraction of ovarian secreted factors was analyzed by mass spectrometry and after proteomic analysis revealed 43 proteins that were known to be secreted. DAVID analysis of biological processes and KEGG pathway analysis indicated that the most represented pathways in the conditioned media were part of the “ECM-related pathways” and “proteoglycans involved in cancer”(Supp. Fig. 5A, B). Of the 43 secreted protein in the correct size, only 7 proteins had EGF-like domains (Fig. 4A). Fibulin1 was reported to inhibit EGFR activity, which would block migration, and it is predicted that fibulin 3 would also be an inhibitor (32). Plau, or urokinase-type plasminogen activator, plays a role

in TGF-β and MMP signaling, but neither inhibitor blocked the pro-migratory impact of the media. Pros1 plays a role in vitamin K mediated clotting. C1sa encodes for complement that mediates innate immunity. Lastly members of the the family (1 and 2) have been linked to ovarian follicle expansion but have not been linked to ovarian cancer. After investigating this list of secreted proteins with the correct molecular weight in the proteomics for both known pro-migration phenotype, known correlation with ovulation, and the ability to stimulate EGFR signaling, only versican met all the criteria. Versican expression correlated with ovarian cancer metastasis, and it was reported to be secreted in the periovulatory stage of rodents during ovulation (13, 20, 24, 33). The presence of secreted versican was validated in the ovarian conditioned media using Western blot (Fig. 4B).

Versican secretion from the ovary is related to the process of ovulation.

Ovulation is a risk factor for ovarian cancer, but few studies have been able to describe the process of ovulation on fallopian tube tumor cell colonization of the ovary. Versican was previously shown to be secreted from the ovary and peak right before ovulation *in vivo* (33); however, these studies have the limitation of being unable to provide the local concentration of versican at the interface of the ovary and the fallopian tube. Using microfluidic technology, we have been able to successfully generate ovulation on platform (19), where we can study the secreted ovarian factors in relation to ovulation and gain more insight into the concentrations and the timing of secretions (Supplemental Figure 6A, B). First, we determined that the ovaries were viable after 8 days in culture on the PREDICT microfluidic system based on calcein green and ethidium red staining (Fig. 4C). Mouse ovaries (day 16–18) were cultured on PREDICT and maintained in FSH (follicle-stimulating hormone) containing media for 6 days. When a group of follicles reached the 400μm diameter, the culture was treated with hCG for 48 hours (human chorionic gonadotropin) (Fig. 4D, E). Expression of versican in the ovaries is shown in supplemental Figure 6C.

Oocyte extrusion and corpus luteum formation were monitored to confirm ovulation by bright field microscopy and hematoxylin/eosin staining respectively (Fig. 4F, G). Media was collected every day from the microfluidic device and analyzed by ELISA to detect estradiol to further confirm ovulation (Fig. 4H) and versican secretion demonstrating a peak of versican in the peri-ovulatory phase (Fig. 4I). Versican was detected by mass spectrometry in conditioned media of ovaries not stimulated to ovulate, but the concentration was unknown. The use of the microfluidic device allowed us to measure the versican concentration in relation to ovulation.

Versican increases migration of fallopian tube cells.

Using purified recombinant versican, we tested increasing concentrations (1–100 ng/ml) of versican on the migration of non-tumorigenic murine (MOE) and human fallopian tube epithelium cells (FT33-TAg). Even at 1 ng/ml, versican significantly increased migration of both cell lines (Fig. 5A, B). Versican also increased migration of MOE cells with TP53 mutations and with PTEN loss (Supp. Fig. 6D, E). Next, we tested whether versican-induced migration was affected by an EGFR inhibitor (PD158780). We found that in both MOE and human FT33-TAg cells, an EGFR inhibitor at 1μM blocked migration induced by recombinant versican even at 100ng/ml (Fig. 5C, D). We also tested erlotinib, a more

selective and clinically used EGFR inhibitor, and demonstrated that erlotinib could inhibit versican induced migration in MOE and FT33-Tag (Fig. 5E, F).

Versican increases invasion and adhesion to the ovary of FTE cells.

After demonstrating that versican is produced by the ovary and stimulates migration, we wanted to address whether versican was able to increase the invasion of fallopian tube cells, which might contribute to ovarian colonization. Boyden chamber assays were performed to investigate invasion. Versican significantly increased invasion of MOE and FT33-Tag. The EGFR inhibitor was able to block invasion stimulated by versican (Fig. 6A–D). To determine if versican could be involved in fallopian tube cells colonizing the ovary, we performed an *ex vivo* adhesion assay where fluorescently labeled MOE or FT33-TAg cells were incubated with murine ovaries with exposed stroma. Our results show that exogenous versican increased fallopian tube adhesion to the ovary in an EGFR-dependent manner (Fig. 6 E–H).

Versican increased EGFR signaling in the fallopian tube.

EGFR activation leads to phosphorylation of AKT and ERK1/2 (34). To confirm that versican was activating these pathways downstream of EGFR signaling, we first treated MOE cells with vehicle, versican or versican plus EGFR inhibitor for 15 and 30 minute and measured phosphorylation of AKT and ERK1/2. Versican increased phosphorylation of AKT (Fig. 7A and C) and ERK (Fig. 7 B and D), which was blocked by EGFR inhibitor. Versican also induced AKT and ERK activation in FT33-Tag (Supplemental Figure 7). The microfluidic system can support the growth of primary oviducts and fallopian tissues for up to 30 days (19, 35). Therefore, we deployed the PREDICT microfluidic platform to perfuse the murine oviductal epithelium and maintained it in a more physiological relevant condition to study versican signaling. Murine oviductal epithelium with residual underlying stroma was used to perform immunofluorescence, and we were able to morphologically distinguish and quantify the fluorescence in the epithelium. Versican stimulated phosphorylation of AKT (Fig. 7 E–F) and ERK (Fig. 7 G–H) in the epithelium in an EGFR-dependent manner.

Conclusions

HGSOC can originate from FTE cells (8, 12, 36) and tumors are detected after they have spread to the ovary (36). The ovary plays a role in high grade serous cancer progression by providing homing factors that can stimulate fallopian tube cells migration (36). Herein, we uncovered the role of the ovarian secreted proteoglycan versican in migration, invasion, and attachment of fallopian tube cells to the ovary. We also found that versican-induced migration, invasion, and ovarian adhesion could be blocked with EGFR inhibitors. Lastly, we recapitulated ovulation using the PREDICT microfluidic organ-on-a-chip platform (19) and demonstrated that ovaries secrete versican over the course of ovulation at concentrations that were sufficient to enhance migration of FTE cells.

This study in consistent with studies showing that versican is important during ovarian cancer metastasis and that it signals through EGFR (37). Versican expression was shown to increase the formation of spheroids in multiple high grade serous cancer cell lines and

shRNA directed against versican significantly reduced peritoneal metastasis indicating that versican may play a role once tumors escape the reproductive tissues. Our study suggests that versican is also important to establish primary metastasis to the ovary. Inhibition of EGFR in ovarian cancer has not been very successful but has only been used after (38) or in combination with platinum-based therapy (39). These clinical trials were based on stratification by EGFR expression, not EGFR activation, however ERK activation is frequent in ovarian cancer without any genetic alterations suggesting that stratification of the patients could be improved and that further studies are needed to understand EGFR signaling in ovarian cancer.

Versican enhances the ability of ovarian cancer cells to induce peritoneal metastasis (13), however, we provide evidence that versican increases pro-migratory and adhesive properties of non-tumorigenic fallopian tube cells to the ovary. Importantly, our data suggested that both wild-type and cells harboring preneoplastic changes, such as the R273 mutation of p53, could respond to versican. Versican exerted a stronger effect on migration in cells with the R273H mutation than in cells expressing the R248W mutation in p53. The literature supports that the R273H induces stronger migration than R248W and that R248W activates different targets (40). Ovarian cancer patients with the R248W mutation show a lower survival due possibly to increased chemoresistance (41, 42). Versican also increased migration of cells with reduced expression of PTEN but did not affect cells expressing the G12V mutation on KRAS. Previous studies have also found that STIC lesions can increase the expression of CD105 and that its expression increases ovarian homing and also impacts their stem-like properties. The mutations that reside in the fallopian tube cell may also play a role in the ability of FTE cells to survive once in the ovarian microenvironment. Data suggests that cell models that lack PTEN are able to survive on 3D collagen surfaces better than non-transformed oviductal cell lines. Therefore, while the ovarian secreted factors may enhance cells with and without preneoplastic changes, the cells may not survive in the ovarian environment unless transformed.

Ex vivo organ culture using organ-on-chip technology has emerged as a technology that allows for the physiological culture of complex tissue systems with perfusion that allows for communication between different organs. Because STIC lesions form only on the fallopian tube fimbria and then ultimately colonize the ovary, studying the local microenvironment between the ovary and the fallopian tube is critical to developing new strategies for prevention and treatment. Further, while other studies have focused on factors in ovarian follicular fluid, the process of ovulation is complex and it is possible that secreted factors from the stroma, granulosa, and theca cells influence the fallopian tube without concentrating in follicular fluid. Tracking the timing and concentration of those factors at the local level in a confined perfusable organ-on-a-chip device, we were able to show that versican correlated with ovulation and was found in physiologically relevant concentrations. These changes were supported by the literature that versican levels are increased in rodents periovulatory and ovulatory phases (33). Others have reported that IGF2 in follicular fluid is capable of full transformation of the fallopian tube (43), which would be interesting to focus on in future investigations to determine if the ovary at ovulation produces specific concentrations that may drive this process. The authors of this study also conclude that the process of ovulation and the role of follicular fluid in reproductive biology is to enhance

migration, invasion and adhesion as part of the ovarian follicle degrading the outer wall of the ovary and enhancing cumulus-oocyte complex movement into the oviduct. Lastly, ovaries in culture produce many secreted factors, but the air-liquid interface allows for the ex vivo cultures to produce estradiol, progesterone, activin A, and activin B in response to gonadotropin stimulation. Using whole ovaries to study fallopian tube colonization involves technical challenges due to the cell lines growing best in liquid but the ovaries requiring an air-liquid interface in a microfluidic. New engineering will be necessary to begin culturing cell lines in direct contact with ovulating ovaries, but will offer important advancements in the modeling of the fimbria-ovarian environment during ovulation.

The prevention of ovarian metastasis could be important for blocking further peritoneal spread. Ovariectomy reduced peritoneal spread and increased survival in two different mouse models of fallopian tube derived HGSOC. Further, intravenous injection of HGSOC cells demonstrates that these cells specifically colonize the ovary providing evidence that secreted factors contribute to this organ-specific homing (27). Allografting cells in the bursa resulted in tumor formation and spread, while grafting the same number of cells into the peritoneal space did not form tumors. Since most patients are diagnosed after widespread peritoneal metastasis the ability to delay or prevent ovarian spread may reduce disease severity. Thus, while many of these cancers are diagnosed late stage, they are actually developing years earlier, which is the primary rationale for the protective role of blocking ovulation on ovarian cancer risk. The entire period of disease progression from p53 signature into a STIC lesion and ultimately HGSOC is thought to take between 7–20 years. Ovulation may play unique roles during each of these processes such as mutation, escape from the fallopian tube, survival as a spheroid as cells shed, and growth of tumor cells within the ovary itself.

In summary (Fig. 8), we found that versican through EGFR stimulates migration, invasion, and adhesion of FTE cells. We also deployed novel organ-on-chip technology to study ovulation and ovarian secreted factors, which confirmed the secretion of versican and provides novel avenues for the study of real-time ovulatory factors on fallopian tube tumorigenesis.

METHODS AND MATERIALS

Cell and tissue culture

Human fallopian tube epithelial cells FT33-TAg were transformed with hTERT and SV40, although non tumorigenic and were a gift from Ronny Drapkin at the University of Pennsylvania (Philadelphia, PA) and murine ovarian epithelial cells MOE were provided by Dr. Barbara Vanderhyden. MOE modified cell lines (p53, PTEN, KRAS) were previously generated in our lab (29) . FT33-TAg cells were maintained in DMEM-Ham's F12 supplemented with penicillin/streptomycin and 2% Ultroser-G (Gibco). MOE cells were grown in the DMEM with 10% FBS (Gibco), L-glutamine (2 mmol/L, Gibco), EGF (0.1 mg/mL, Roche), ITS (Roche), gentamicin (50 mg/mL, Gibco), estradiol (1 mg/mL in 100% EtOH, Sigma Aldrich) and penicillin/streptomycin. Cells were passaged a maximum of 20 times and cultured in the monolayers in 5% CO_2 at 37 °C cell incubator. Oviducts were grown in growth media (50% αMEM, 50% DMEM/F12, 0.3% BSA, 5μg/ml ITS, 1%

Penicillin/streptomycin, 50mg/L Gentamicin). Ovaries from pre-pubertal mice were grown in growth media plus 10mg/ml fetuin and 10mIU/ml FSH for 6–7 days (or until follicles were about 400μm, then the media was replaced with maturation media (50% αMEM, 50% DMEM/F12, 10% FBS, 10 ng/ml EGF, 1% Penicillin/streptomycin, 50mg/L Gentamicin) plus 1.5UI/ml hCG and 10mUI/ml FSH.

Ovary organoid culture and conditioned media collection

All animals were treated in accordance with NIH Guidelines for the Care and Use of Laboratory Animals and the established Institutional Animal Use and Care protocol at the University of Illinois (Chicago, IL). CD1 mice were housed under normal condition environment and provided food and water. Ovaries and fallopian tubes were collected after 16 days from new pups born in dissection medium (Leibovitz's plus 1% penicillin/ Streptomycin). In briefly, the 0.5% (w/v) alginate was diluted in sterile PBS and maintained at 37°C beforehand. Dissection and culture media were heated to 37 °C. Ovaries and fallopian tubes were collected and transferred to dissection media, where the ovaries were cut into 2 halves. The ovaries were then placed into a single alginate droplet onto a sterilized mesh fiber with a syringe and inverted to allow gravity to force the alginate into a hanging drop. The drop was then released in a 10cm dish containing 10mM $CaCl_2$ solution (37 °C) to polymerize the alginate into a gel. After incubation for another 2 minutes, the ovaries were transferred to αMEM culture medium and incubated at 37 °C for 48 hours before collecting the conditioned media.

Ovulation on PREDICT microfluidic system

Ovaries from pre-pubertal mice of 16 days of age were dissected from the reproductive tract and cut in 4 sections. The ovaries were added to the wells of the 35-well tissue plate that was prior washed with PBS and growth media containing 10 mUI/ml of FSH is added into the donor reservoir and excess/conditioned media is pumped into the acceptor reservoir with a flow of 40 μl/hour. Every day the conditioned media is collected for analysis and saved at −80 °C. After 7 days, the follicles reached the 400 μm diameter, maturation media containing 1.3 IU/ml hCG is added for 2–3 days. After the experiments, the tissue plate is detached from the pump plate and washed with distilled water and then with 5% Ethanol for 30 min. The pump plate is washed with 1% tergazyme solution that is disposed in a reservoir at the bottom of the pump plate for 1 hour surge. The solution is removed and washed 3 times with distilled water following 70% ethanol surge wash using the surge function. The plate is dried in the hood overnight (1).

Immunofluorescence of oviducts

Oviduct were dissected from murine reproductive systems; epithelium was isolated and inserted into PREDICT well plates. Growth media was added to the donor well with the treatments indicated. Media was changed every day. After 72hrs, tissues were collected and fixed in 4% PFA, washed with PBS and permeabilized/blocked with PBS +0.1% Triton-X100 and goat serum for 1hr at R.T. The day after tissues were incubated with primary antibodies targeting pAKT or pERK overnight at 4°C.

Tissues were then washed in PBS 3X, incubated with DAPI for 15 min, washed and mounted with anti-fade mounting media. At least 3 oviducts per treatment were stained, imaged and fluorescence was quantified using Image J.

Live/Dead staining

The tissues were cultivated on transwell and transferred to 96 well plates for staining. Live green (calcein AM/Component A) and Dead red (ethidium homodimer-1/Component B) (Invitrogen kit no#) were thawed and Live green was transferred into Dead red to create a 2x staining solution as per kit instructions. Medium was removed from tissues and a 1x solution of live/dead staining solution in PBS was added directly to cells or tissue. After incubation for 15 minutes at 20–25°C, the tissue was transferred to a slide, and a coverslip was used to further flatten the tissue. The tissue was immediately imaged using a fluorescence microscope.

Mass spectrometry proteomic identification

Conditioned media from three biological replicates was isolated and 5 μg protein from conditioned medium were denatured by adding 8M urea and incubating at 50°C for 60 min. Subsequently, proteins were reduced by adding 10mM DTT (final concentration 1mM) and incubating at 50° C for 15 min. Alkalinization was then obtained by adding 100 mM Iodoacetamide (final concentration 10mM) and incubating in dark at room temperature for 15 min. The protein sample was then digested by diluting from 8M to 1M urea by adding 100mM ammonium bicarbonate and trypsin. The sample was digested at 37° C overnight. The digested samples were desalted using reverse phase C18 spin columns (Thermo Fisher Scientific, Rockford, IL) and peptides were concentrated *in vacuum*. Dried peptides were suspended in 5% acetonitrile and 0.1% formic acid. The samples were loaded directly onto a 15 cm long, 75 μM reversed phase capillary column (ProteoPep™ II C18, 300 Å, 5 μm size, New Objective, Woburn MA) and separated with a 200-minute gradient from 5% acetonitrile to 100% acetonitrile on a Proxeon Easy n-LC II (Thermo Scientific, San Jose, CA). The peptides were directly eluted into an LTQ Orbitrap Velos mass spectrometer (Thermo Scientific, San Jose, CA) with electrospray ionization at 350 nl/minute flow rate. The mass spectrometer was operated in data dependent mode, and for each MS1 precursor ion scan the ten most intense ions were selected from fragmentation by CID (collision induced dissociation). The other parameters for mass spectrometry analysis were: resolution of MS1 was set at 60,000, normalized collision energy 35%, activation time 10 ms, isolation width 1.5, and +4 and higher charge states were rejected.

Immunoblot analysis

Cell lysates were prepared using RIPA lysis buffer (50 mmol/L Tris pH 7.6, 150 mmol/L NaCl, 1% Triton X-100, 0.1% SDS) supplemented with protease (Roche Applied Science #4693159001) and phosphatase (Sigma-Aldrich #P0044) inhibitors. Concentration of proteins in lysates was determined by Bradford Assay (Bio-Rad #5000205) normalized under standard curve and proteins were resolved on SDS-PAGE gel. After that, proteins were transferred to nitrocellulose membrane and blocked in 5% nonfat milk. Primary antibodies including of EGFR (4267, CST; AB_2864406), versican (ab19345, Abcam; AB_444865) and GAPDH (2118, CST) were incubated with the membrane overnight

at 4°C. Membrane was washed and incubated with goat anti-rabbit or goat anti-mouse secondary antibody conjugated with horseradish peroxidase (HRP) (anti-rabbit IgG, HRP-linked antibody 7074 or anti-mouse IgG, HRP-linked Antibody 7076). After incubation, the membranes were washed three times, protein bands were detected with SuperSignal West Femto Substrate (Thermo Fisher Scientific, 34095) and imaged on a FluorChem E System (ProteinSimple).

Wound healing assay for cell migration

Cells were seeded at 50,000 cells per well in 24-well plate. Briefly, scratch was made, medium removed and substituted with medium containing vehicle or ovary conditioned media, recombinant proteins, or chemical compounds. Pictures were taken right after the scratch and 24 hours later using an AmScope MU900 with Toupview software (AmScope, Irvine, CA). The percent rate (%) of disclosure was calculated based on the statistics of Image J software.

Boyden chamber assay for cell invasion

Matrigel was thawed out on ice and diluted to 300 μg/ml with serum-free medium. 120 μl of diluted Matrigel was dropped to the 8 μm inserts of the Boyden chamber and incubated at 37°C for at least 1hr to solidify. 500μl of complete medium was added to at the bottom of each well in 24-well plate. Treated cells were trypsinized and collected in media before PBS washing (twice), resuspended in 120 μl serum-free medium and incubated for 24 hours. At the end of incubation, cotton swab was applied to remove the cells in top of insert following with 4% PFA fixing for 5 min, permeabilization with 70% methanol, and stained with 0.2% crystal violet 10% ethanol mixed solution for 10 min. Inserts were then rinsed twice with PBS and dried overnight. Images of each insert were taken using AmScope MU900 with Toupview software (AmScope, Irvine, CA) and invading cells (at the bottom of the insert) were quantified in ImageJ software.

Ex vivo colonization assay

For MOE cells, the assay was performed as described earlier (28, 30). Briefly, MOE cells stably expressing RFP were incubated with ovaries from 16–17 days old CD1 mice. The ovaries were wounded with a scalpel blade to mimic ovulation and each ovary was incubated with 30,000 fluorescently labeled cells. For FT33-TAg, labeling of the cells was done using CellTracker (C7025, Invitrogen) at 0.5μM final concentration for 30min on trypsinized cells. Cells were incubated with ovaries overnight at 37°C in an orbital shaker (40 rpm). The next day ovaries were washed several times, observable cells were counted, and representative pictures were taken with an AmScope MU900 with Toupview software (AmScope, Irvine, CA). At least three independent experiments were performed, each with 3 replicates and statistical analysis was performed using one-way ANOVA.

Immunohistochemistry (IHC)

Tissues were fixed in 4% PFA, embedded in paraffin, processed, and prepared for immunohistochemistry as previously reported (10, 44, 45). Primary antibodies were

incubated overnight. Images were acquired on a Nikon Eclipse E600 microscope using a DS-Ri1 digital camera and NIS Elements software.

ELISA

Conditioned media was collected every day and stored at −80°C until completion of the experiment. Standard and samples were prepared as described in the manufacturer's instruction for Estradiol ELISA (Cayman, 501890) and Versican ELISA (Abclonal, RK03285).

Proliferation assay

A total of 3,000 cells were plated in triplicates in a clear flat–bottom 96 plate and allowed to attach overnight. Control, ovarian or fallopian tube conditioned media was added to the cells for zero, 2, 4 and 6 days. Cell viability was determined using 0.04% Sulforhodamine B via colorimetric detection of proteins at 505nm as previously described (46).

Statistical analyses

All experiments were performed in were performed in duplicate or triplicate technical replicates and subsequently repeated in at least 3 independent biological replicates. For the biological replicates, each time cells were seeded at different days and processed independently. For tissues, mice from different litters were used.

Data presented are as MEAN±SEM represent three or more independent experiments or biological replicates. Statistical analysis was carried out using GraphPad Prism 7 software. Statistical significance was determined by Student unpaired t-test or one-way ANOVA followed by a Tukey's post-hoc analysis. NS means no significant difference; *, $P < 0.05$; **, $P < 0.01$; ***, $P < 0.001$; ****, $P < 0.0001$ means existing significant difference as indicated.

Supplementary Material

Refer to Web version on PubMed Central for supplementary material.

Acknowledgements

Research supported in this publication was supported by the National Institute of Health under Award Number R01CA240301 and R01CA240423. The content is solely the responsibility of the authors and does not necessarily represent the officials' views of the National Institute of Health.

References

1. Azizgolshani H, Coppeta JR, Vedula EM, Marr EE, Cain BP, Luu RJ, et al. High-throughput organ-on-chip platform with integrated programmable fluid flow and real-time sensing for complex tissue models in drug development workflows. Lab Chip. 2021;21(8):1454–74. [PubMed: 33881130]
2. Singh N, McCluggage WG, Gilks CB. High-grade serous carcinoma of tubo-ovarian origin: recent developments. Histopathology. 2017;71(3):339–56. [PubMed: 28477361]
3. Matsuo K, Machida H, Grubbs BH, Sood AK, Gershenson DM. Trends of low-grade serous ovarian carcinoma in the United States. J Gynecol Oncol. 2018;29(1):e15. [PubMed: 29185273]

4. Perets R, Wyant GA, Muto KW, Bijron JG, Poole BB, Chin KT, et al. Transformation of the fallopian tube secretory epithelium leads to high-grade serous ovarian cancer in Brca;Tp53;Pten models. Cancer Cell. 2013;24(6):751–65. [PubMed: 24332043]
5. Roh MH, Yassin Y, Miron A, Mehra KK, Mehrad M, Monte NM, et al. High-grade fimbrial-ovarian carcinomas are unified by altered p53, PTEN and PAX2 expression. Mod Pathol. 2010;23(10):1316–24. [PubMed: 20562848]
6. Falconer H, Yin L, Gronberg H, Altman D. Ovarian cancer risk after salpingectomy: a nationwide population-based study. J Natl Cancer Inst. 2015;107(2).
7. Fathalla MF. Incessant ovulation and ovarian cancer - a hypothesis re-visited. Facts Views Vis Obgyn. 2013;5(4):292–7. [PubMed: 24753957]
8. Labidi-Galy SI, Papp E, Hallberg D, Niknafs N, Adleff V, Noe M, et al. High grade serous ovarian carcinomas originate in the fallopian tube. Nat Commun. 2017;8(1):1093. [PubMed: 29061967]
9. Bahar-Shany K, Brand H, Sapoznik S, Jacob-Hirsch J, Yung Y, Korach J, et al. Exposure of fallopian tube epithelium to follicular fluid mimics carcinogenic changes in precursor lesions of serous papillary carcinoma. Gynecol Oncol. 2014;132(2):322–7. [PubMed: 24355484]
10. King SM, Hilliard TS, Wu LY, Jaffe RC, Fazleabas AT, Burdette JE. The impact of ovulation on fallopian tube epithelial cells: evaluating three hypotheses connecting ovulation and serous ovarian cancer. Endocr Relat Cancer. 2011;18(5):627–42. [PubMed: 21813729]
11. Zhang S, Dolgalev I, Zhang T, Ran H, Levine DA, Neel BG. Both fallopian tube and ovarian surface epithelium are cells-of-origin for high-grade serous ovarian carcinoma. Nat Commun. 2019;10(1):5367. [PubMed: 31772167]
12. Kyo S, Ishikawa N, Nakamura K, Nakayama K. The fallopian tube as origin of ovarian cancer: Change of diagnostic and preventive strategies. Cancer Med. 2020;9(2):421–31. [PubMed: 31769234]
13. Desjardins M, Xie J, Gurler H, Muralidhar GG, Sacks JD, Burdette JE, et al. Versican regulates metastasis of epithelial ovarian carcinoma cells and spheroids. J Ovarian Res. 2014;7:70. [PubMed: 24999371]
14. Dean M, Davis DA, Burdette JE. Activin A stimulates migration of the fallopian tube epithelium, an origin of high-grade serous ovarian cancer, through non-canonical signaling. Cancer Lett. 2017;391:114–24. [PubMed: 28115208]
15. Gjyshi A, Dash S, Cen L, Cheng CH, Zhang C, Yoder SJ, et al. Early transcriptional response of human ovarian and fallopian tube surface epithelial cells to norepinephrine. Sci Rep. 2018;8(1):8291. [PubMed: 29844388]
16. Zink KE, Dean M, Burdette JE, Sanchez LM. Imaging Mass Spectrometry Reveals Crosstalk between the Fallopian Tube and the Ovary that Drives Primary Metastasis of Ovarian Cancer. ACS Cent Sci. 2018;4(10):1360–70. [PubMed: 30410974]
17. Kang M, Chong KY, Hartwich TMP, Bi F, Witham AK, Patrick D, et al. Ovarian BDNF promotes survival, migration, and attachment of tumor precursors originated from p53 mutant fallopian tube epithelial cells. Oncogenesis. 2020;9(5):55. [PubMed: 32471985]
18. Bai S, Zhu W, Coffman L, Vlad A, Schwartz LE, Elishaev E, et al. CD105 Is Expressed in Ovarian Cancer Precursor Lesions and Is Required for Metastasis to the Ovary. Cancers (Basel). 2019;11(11).
19. Xiao S, Coppeta JR, Rogers HB, Isenberg BC, Zhu J, Olalekan SA, et al. A microfluidic culture model of the human reproductive tract and 28-day menstrual cycle. Nat Commun. 2017;8:14584.
20. Voutilainen K, Anttila M, Sillanpaa S, Tammi R, Tammi M, Saarikoski S, et al. Versican in epithelial ovarian cancer: relation to hyaluronan, clinicopathologic factors and prognosis. Int J Cancer. 2003;107(3):359–64. [PubMed: 14506734]
21. Ween MP, Oehler MK, Ricciardelli C. Role of versican, hyaluronan and CD44 in ovarian cancer metastasis. Int J Mol Sci. 2011;12(2):1009–29. [PubMed: 21541039]
22. Ween MP, Hummitzsch K, Rodgers RJ, Oehler MK, Ricciardelli C. Versican induces a pro-metastatic ovarian cancer cell behavior which can be inhibited by small hyaluronan oligosaccharides. Clin Exp Metastasis. 2011;28(2):113–25. [PubMed: 21153687]
23. Cho A, Howell VM, Colvin EK. The Extracellular Matrix in Epithelial Ovarian Cancer - A Piece of a Puzzle. Front Oncol. 2015;5:245. [PubMed: 26579497]

24. Ghosh S, Albitar L, LeBaron R, Welch WR, Samimi G, Birrer MJ, et al. Up-regulation of stromal versican expression in advanced stage serous ovarian cancer. Gynecol Oncol. 2010;119(1):114–20. [PubMed: 20619446]
25. Salem M, O'Brien JA, Bernaudo S, Shawer H, Ye G, Brkic J, et al. miR-590–3p Promotes Ovarian Cancer Growth and Metastasis via a Novel FOXA2-Versican Pathway. Cancer Res. 2018;78(15):4175–90. [PubMed: 29748371]
26. Yee AJ, Akens M, Yang BL, Finkelstein J, Zheng PS, Deng Z, et al. The effect of versican G3 domain on local breast cancer invasiveness and bony metastasis. Breast Cancer Res. 2007;9(4):R47. [PubMed: 17662123]
27. Coffman LG, Burgos-Ojeda D, Wu R, Cho K, Bai S, Buckanovich RJ. New models of hematogenous ovarian cancer metastasis demonstrate preferential spread to the ovary and a requirement for the ovary for abdominal dissemination. Transl Res. 2016;175:92–102 e2.
28. Dean M, Jin V, Russo A, Lantvit DD, Burdette JE. Exposure of the extracellular matrix and colonization of the ovary in metastasis of fallopian-tube-derived cancer. Carcinogenesis. 2019;40(1):41–51. [PubMed: 30475985]
29. Eddie SL, Quartuccio SM, Oh E, Moyle-Heyrman G, Lantvit DD, Wei JJ, et al. Tumorigenesis and peritoneal colonization from fallopian tube epithelium. Oncotarget. 2015;6(24):20500–12. [PubMed: 25971410]
30. Russo A, Czarnecki AA, Dean M, Modi DA, Lantvit DD, Hardy L, et al. PTEN loss in the fallopian tube induces hyperplasia and ovarian tumor formation. Oncogene. 2018.
31. Quartuccio SM, Karthikeyan S, Eddie SL, Lantvit DD, E Oh, Modi DA, et al. Mutant p53 expression in fallopian tube epithelium drives cell migration. Int J Cancer. 2015;137(7):1528–38. [PubMed: 25810107]
32. Harikrishnan K, Joshi O, Madangirikar S, Balasubramanian N. Cell Derived Matrix Fibulin-1 Associates With Epidermal Growth Factor Receptor to Inhibit Its Activation, Localization and Function in Lung Cancer Calu-1 Cells. Front Cell Dev Biol. 2020;8:522. [PubMed: 32719793]
33. Russell DL, Ochsner SA, Hsieh M, Mulders S, Richards JS. Hormone-regulated expression and localization of versican in the rodent ovary. Endocrinology. 2003;144(3):1020–31. [PubMed: 12586779]
34. Gan Y, Shi C, Inge L, Hibner M, Balducci J, Huang Y. Differential roles of ERK and Akt pathways in regulation of EGFR-mediated signaling and motility in prostate cancer cells. Oncogene. 2010;29(35):4947–58. [PubMed: 20562913]
35. Zhu J, Xu Y, Rashedi AS, Pavone ME, Kim JJ, Woodruff TK, et al. Human fallopian tube epithelium co-culture with murine ovarian follicles reveals crosstalk in the reproductive cycle. Mol Hum Reprod. 2016;22(11):756–67. [PubMed: 27542947]
36. Bergsten TM, Burdette JE, Dean M. Fallopian tube initiation of high grade serous ovarian cancer and ovarian metastasis: Mechanisms and therapeutic implications. Cancer Lett. 2020;476:152–60. [PubMed: 32067992]
37. Wu YJ, La Pierre DP, Wu J, Yee AJ, Yang BB. The interaction of versican with its binding partners. Cell Res. 2005;15(7):483–94. [PubMed: 16045811]
38. Gordon AN, Finkler N, Edwards RP, Garcia AA, Crozier M, Irwin DH, et al. Efficacy and safety of erlotinib HCl, an epidermal growth factor receptor (HER1/EGFR) tyrosine kinase inhibitor, in patients with advanced ovarian carcinoma: results from a phase II multicenter study. Int J Gynecol Cancer. 2005;15(5):785–92. [PubMed: 16174225]
39. Vergote IB, Jimeno A, Joly F, Katsaros D, Coens C, Despierre E, et al. Randomized phase III study of erlotinib versus observation in patients with no evidence of disease progression after first-line platin-based chemotherapy for ovarian carcinoma: a European Organisation for Research and Treatment of Cancer-Gynaecological Cancer Group, and Gynecologic Cancer Intergroup study. J Clin Oncol. 2014;32(4):320–6. [PubMed: 24366937]
40. Karthikeyan S, Lantvit DD, Chae DH, Burdette JE. Cadherin-6 type 2, K-cadherin (CDH6) is regulated by mutant p53 in the fallopian tube but is not expressed in the ovarian surface. Oncotarget. 2016;7(43):69871–82. [PubMed: 27563818]
41. Brachova P, Thiel KW, Leslie KK. The consequence of oncomorphic TP53 mutations in ovarian cancer. Int J Mol Sci. 2013;14(9):19257–75.

42. Seagle BL, Eng KH, Dandapani M, Yeh JY, Odunsi K, Shahabi S. Survival of patients with structurally-grouped TP53 mutations in ovarian and breast cancers. Oncotarget. 2015;6(21):18641–52.

43. Hsu CF, Huang HS, Chen PC, Ding DC, Chu TY. IGF-axis confers transformation and regeneration of fallopian tube fimbria epithelium upon ovulation. EBioMedicine. 2019;41:597–609. [PubMed: 30852161]

44. Eddie SL, Quartuccio SM, Oh E, Moyle-Heyrman G, Lantvit DD, Wei JJ, et al. Tumorigenesis and peritoneal colonization from fallopian tube epithelium. Oncotarget. 2015.

45. King SM, Quartuccio SM, Vanderhyden BC, Burdette JE. Early transformative changes in normal ovarian surface epithelium induced by oxidative stress require Akt upregulation, DNA damage and epithelial-stromal interaction. Carcinogenesis. 2013;34(5):1125–33. [PubMed: 23299406]

46. Vichai V, Kirtikara K. Sulforhodamine B colorimetric assay for cytotoxicity screening. Nat Protoc. 2006;1(3):1112–6. [PubMed: 17406391]

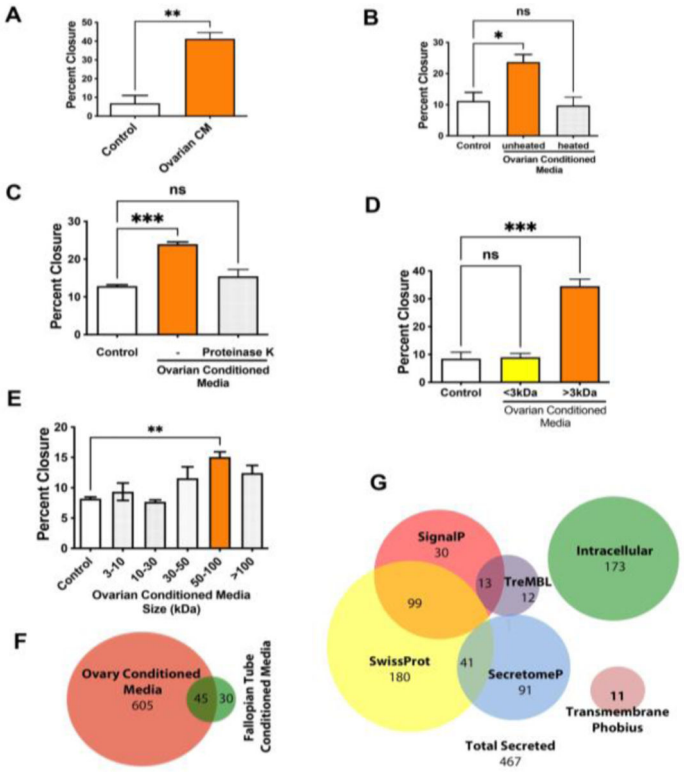

Figure 1: Secreted proteins from the ovary increase the migratory ability of fallopian tube epithelial cells.

(A) Wound healing assay analysis for the migration of MOE cells incubated with ovarian conditioned media (CM) for 24h. (B) Wound healing assay after heat at 70°C for 10 min or (C) proteinase K (100μg/mL)-treated conditioned media. (D, E) Migration of MOE cells incubated with ovary conditioned media fractioned by different size of filters, including of 3–10, 10–30, 30–50, 50–100, >100 kDa. (F) Venn diagram comparing the proteins in the ovarian conditioned media to fallopian tube conditioned medium. (G) Venn diagrams showing overlap with proteomics and predicted secreted proteins. A minimum of three independent experiments, biological replicates were analyzed using one-way ANOVA (ns>0.05, p*<0.05, p**<0.01, p***<0.001).

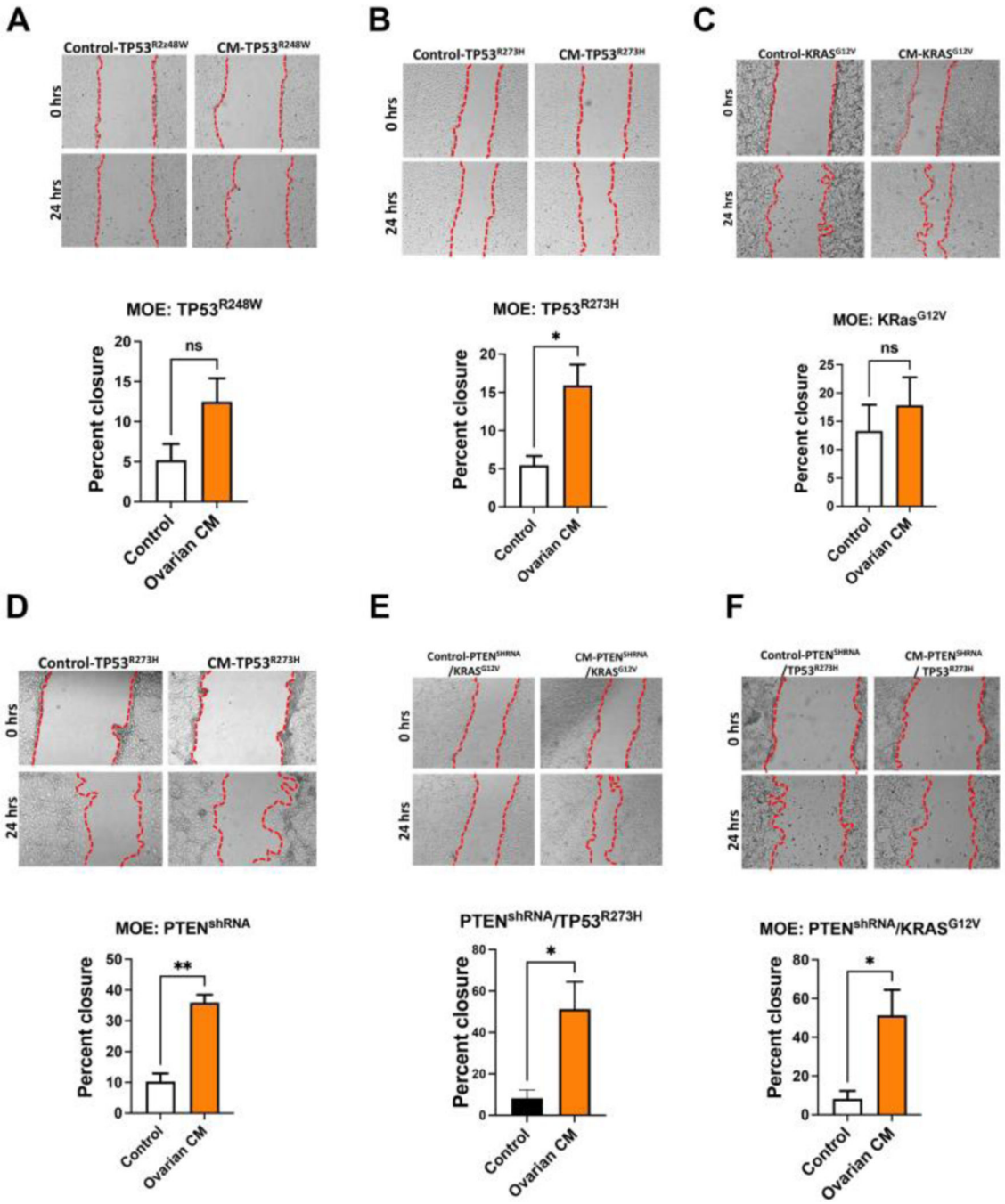

Figure 2: Secreted factors from the ovary increase the migration in fallopian tube models of early tumorigenesis.

(A) Wound healing assay analysis for the migration of MOE cells stably transfected with p53 mutant R248, (B) p53 mutant R273H, (C) RAS G12V, (D) shRNA targeting PTEN, (E) shRNA targeting PTEN + TP53 mutant R273H and (F) shRNA targeting PTEN + RAS G12V in response to ovarian conditioned media stimulation for 24h. A minimum of three independent experiments, biological replicates were analyzed using T-test (p*<0.05, p**<0.01).

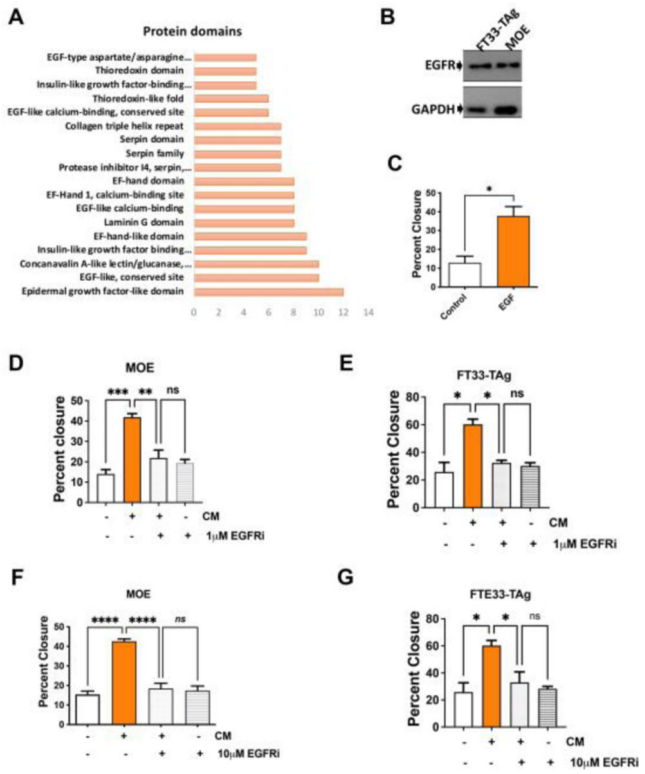

Figure 3: Ovarian conditioned media increases fallopian tube cell migration in an EGFR-dependent manner.

(A) DAVID protein domain analysis shows enriched proteins containing EGF-like domains. (B) Western blot analysis detecting EGFR expression in human (FT33-TAg) and murine (MOE) fallopian tube epithelial cells. (C) Wound healing assay in MOE cells treated with recombinant EGF (concentration) for 24h. (D) Wound healing assay in MOE cells and (E) FT33-TAg cells treated with conditioned media −/+ 1 μM of EGFR inhibitor PD158780 for 24hrs. Wound healing assay in (F) MOE and (G) FT33-TAg treated with conditioned media −/+ 10 μM of EGFR inhibitor PD158780. A minimum of three independent experiments, biological replicates were analyzed using one-way ANOVA (ns>0.05, p*<0.05, p**<0.01, p***<0.001, p****<0.0001).

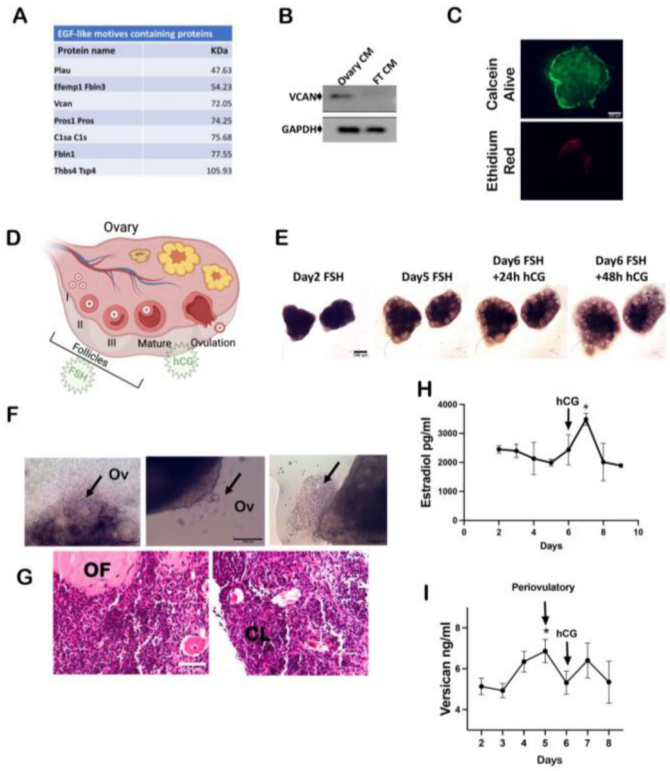

Figure 4: The EGF-like domain containing proteoglycan versican is secreted during ovulation in a 3D dynamic culture.

(A) Table showing proteins between 50–100 kDa containing EGF-like domains that were identified in ovarian conditioned media through mass spectrometry. (B) Western blot analysis of versican expression in medium conditioned with ovary and fallopian tube (FT) (CM=conditioned media). (C) Live/Dead staining using permeable calcein dye (green) and ethidium red (red). (D) Schematic of ovulation induced by FSH/hCG stimulation. (E) Bright field images of ovarian follicles growth during the treatment for 6 days treatment with FSH. (F) Bright field images of ovulating follicles. Black arrow pointing at oocytes extrusion. (G) Hematoxylin & Eosin staining showing follicles maturation. Ov=ovulation; OF= ovulated follicle; CL= corpus luteum. (H) ELISA detecting estradiol levels in conditioned media collected during the *ex vivo* dynamic ovulation on PREDICT. (I) ELISA detecting versican levels in conditioned media collected during the *ex vivo* dynamic ovulation on PREDICT. A minimum of three independent experiments, biological replicates were analyzed using one-way ANOVA (p*<0.05).

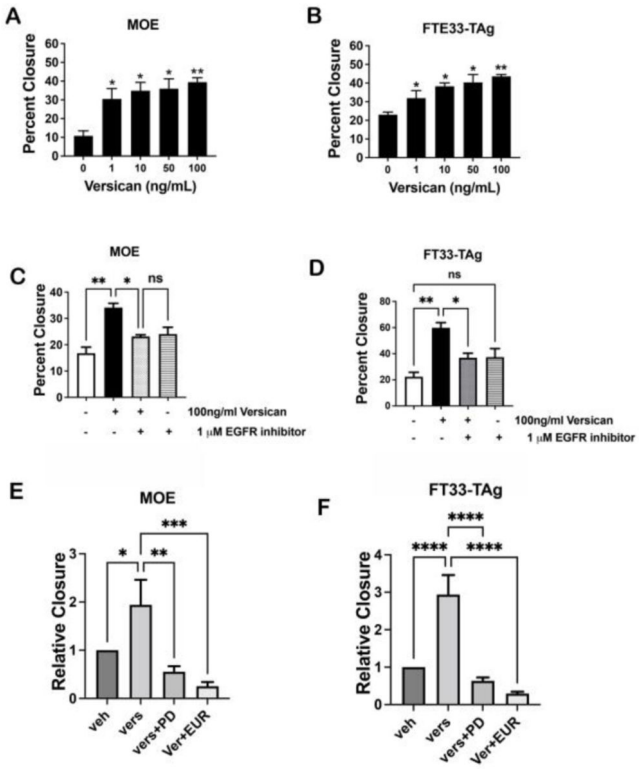

Figure 5: Versican secreted from the ovary drives migration of fallopian tube epithelial cells.

Migration analysis of (A) MOE and (B) FT33-TAg cells treated with human recombinant versican (0–100 ng/ml) after 24h. Wound healing assay in (C) MOE and (D) FTE 33Tag cells treated with versican and 1 μM EGFR inhibitor after 24h. Migration analysis of MOE cells (E) and FT33-Tag (F) incubated with recombinant versican for 24h with and without EGFR inhibitors PD158780 10 μM or Erlotinib 10 μM (EUR). A minimum of three independent experiments, biological replicates were analyzed using one-way ANOVA (ns>0.05, p*<0.05, p**<0.01, ***, ****).

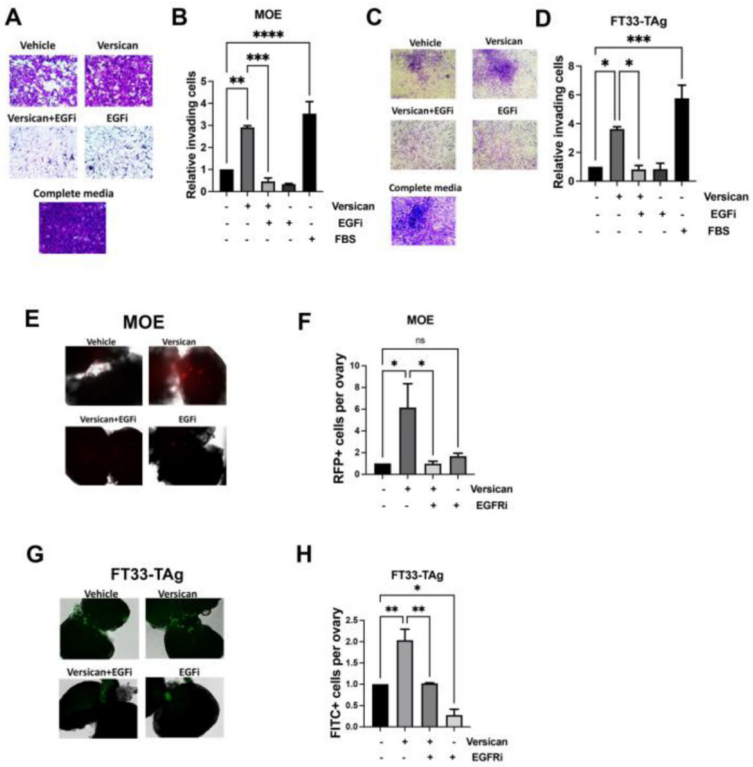

Figure 6: Versican increases invasion and adhesion to the ovary in an EGFR-dependent manner.

Boyden chamber invasion assay of (A-B) MOE cells and FT33-TAg cells (C-D) incubated with versican 100 ng/ml for 24h −/+ EGFR inhibitor (EGFRi) 1 μM. Adhesion to the ovary of fluorescently labeled MOE cells (E and G) FT33-TAg cells (F and H) after treatment with versican 100 ng/ml for 24h −/+ EGFR inhibitor 1 μM. A minimum of three independent experiments, biological replicates were analyzed using one-way ANOVA (ns>0.05, p*<0.05, p**<0.01, p***<0.001, P****<0.0001).

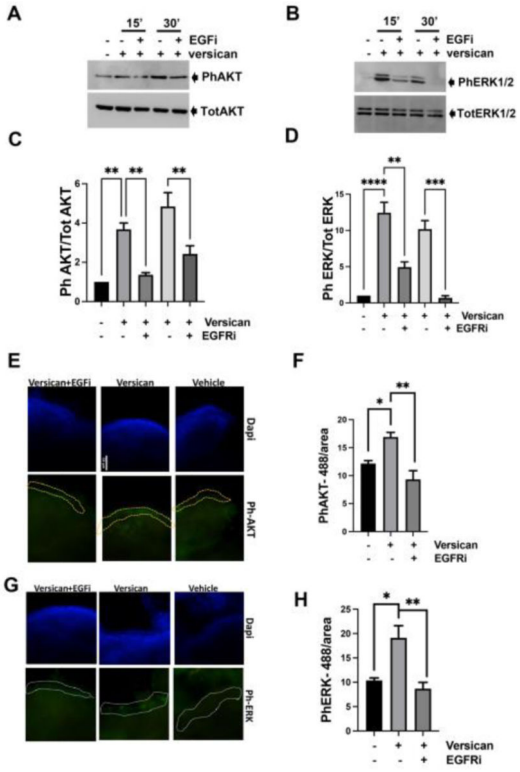

Figure 7: Versican activates EGFR signaling in fallopian tube epithelium cells.

Western blot analysis of phosphorylated AKT and phosphorylated ERK1/2 using specific antibodies in MOE cells (A-C) and FTE 33-Tag cells (B-D) incubated with versican 100 ng/ml for 15 and 30 minutes −/+ EGFR inhibitor 1 μM. Immunofluorescence analysis of phosphorylated AKT (E-F) and phosphorylated ERK1/2 (G-H) using specific antibodies in murine oviductal organs cultured in the PREDICT microfluidic device. A minimum of three independent experiments, biological replicates were analyzed using one-way ANOVA (ns>0.05, p*<0.05, p**<0.01, p***<0.001, P****<0.0001).

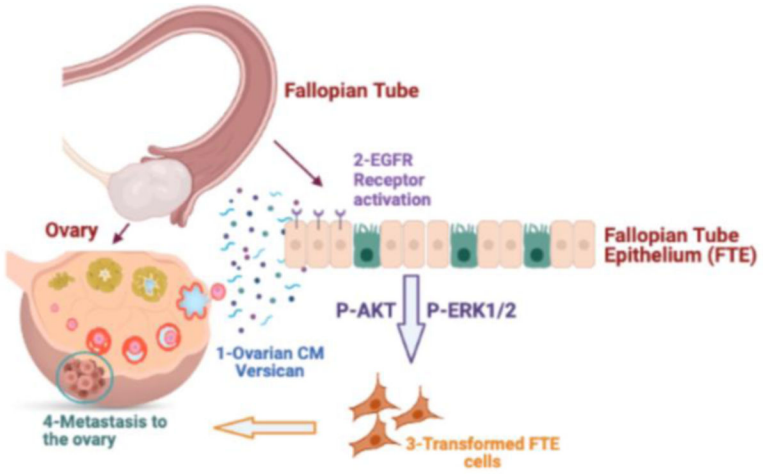

Figure 8. Schematic of versican function.

1) Versican is released during ovulation and 2) binds EGFR on fallopian tube cells leading to activation of the receptor and phosphorylation of AKT and ERK1/2. This signaling pathways increase the migration, invasion, and adhesion of FTE during ovarian colonization.